Thermal Effects and Scaling in Organic Light-Emitting Flat-Panel Displays

James C. Sturm, *Senior Member, IEEE,* Wendy Wilson, and Mario Iodice

(Invited Paper)

Abstract—The temperature rise in flat-panel displays without forced air cooling has been both modeled and experimentally measured as a function of the display size. Both radiation and convection are important processes for the transfer of heat to the ambient. Because of much poorer convection and the lack of lateral heat transport at large dimensions, for a fixed power density large displays are expected to be substantially hotter than small displays. This could adversely impact the reliability of large displays based on organic light-emitting diode (OLED) technology.

Index Terms—Convection, flat-panel displays, heating, organic light emitting device, radiation, thermal effects.

LIST OF SYMBOLS

A	Display area.
β	Thermal expansion coefficient of air.
c_p	Specific heat of air.
ε	Display emissivity.
g	Gravitational constant.
G_T	Thermal conductance.
h_c	Surface heat transfer coefficient for convection.
$h_{\mathrm{avg,tot}}$	Average total surface heat transfer coefficient.
h_r	Surface heat transfer coefficient for radiation.
η_I	Luminous current efficiency.
η_L	Luminous power efficiency.
k_a	Thermal conductivity of air.
k_g	Thermal conductivity of glass.
L	Luminance.
Lc	Display critical dimension.
L_D	Display size.
μ	Viscosity of air.
Nu	Nusselt number.
P	Power.
Pe	Display perimeter.
Pr	Prandtl number.
Ra	Rayleigh number.
ρ	Density of air.
t	Display thickness.
T_A	Temperature of the ambient.
T_D	Temperature of the display surface.
ΔT_D	Increase in temperature of the display from ambient.

J. C. Sturm is with the Center for Photonics and Optoelectronic Materials, Department of Electrical Engineering, Princeton University, Princeton, NJ 08544 USA.

W. Wilson was with Center for Photonics and Optoelectronic Materials, Department of Electrical Engineering, Princeton University, Princeton, NJ 08544 USA. She is now with the Department of Physics, University of Utah, Salt Lake City, UT 84112 USA.

M. Iodice was with the Center for Photonics and Optoelectronic Materials, Department of Electrical Engineering, Princeton University, Princeton, NJ 08544 USA. He is now with the IRECE-National Council of Research, 80124 Naples, Italy.

I. INTRODUCTION

SINCE THE seminal work of Tang and Van Slyke [1] there has been an increasingly strong interest in developing flat-panel displays based on organic LED's (OLED's), either based on polymers or small organic molecules [2]–[4]. Two critical issues for applications involving either class of material are the thermal stability of the LED structure and the reliability of the devices, which is also expected to depend on their temperature [5]–[8]. In addition to depending on the ambient temperature, the temperature of the organic devices will also depend on self-heating due to the power dissipation of the devices themselves. In this paper, we experimentally measure self-heating effects and model the rise in the temperature of a display consisting of a flat plate of glass as a function of size, orientation, and power density. Only passive cooling and no active cooling such as fans, thermoelectric coolers, etc., are considered. We find that it is easily possible to have temperature rises of many tens of degrees under technologically relevant conditions, and that large displays will be much hotter than small displays for a fixed brightness (and thus fixed power density).

II. POWER DISSIPATION IN ORGANIC FLAT-PANEL DISPLAYS

In this section, we make some estimates of the actual power dissipation in future OLED display products, based on published reports of device performance. Assuming a Lambertian angular distribution of emitted light, the luminous power efficiency of a display (η_L, expressed in lumens/watt, lm/W) is related to its current efficiency (η_I, expressed in candelas/ampere, cd/A) as

$$\eta_L = \pi \eta_I / V_D \tag{1}$$

where V_D is the drive voltage on the OLED. In practice, η_I is often constant over wide ranges of operation, so that η_L decreases as the current level and, hence, drive voltage increase. Typical current efficiencies (in the blue and green) range from 2 to 10 cd/A, and drive voltages for 100 cd/m^2 range from 3 to 10 V. Therefore, a typical luminous efficiency (η_L) at a luminance (L) of 100 cd/m^2 ranges from under 1 to ~10 lm/W. Assuming an average display luminance (brightness) of 100 cd/m^2, corresponding to 314 lm/m^2, and choosing a luminous efficiency of 3 lm/W, the display power dissipation would be ~100 W/m^2 when all pixels are on, which is certainly possible in many applications.

In a system application, however, there are several other factors which will considerably increase this number. The first is that a high contrast display is typically required, whereas an OLED is a very reflective device because of the transparency of the organic and high reflectivity of the metal cathode. The most straightforward solution chosen by several groups is to put a circular polarizer in front of the display, which greatly reduces reflected light to improve contrast. While this ideally leads to a 50% reduction in the emitted light, in practice this emitted light is only ~40% of the original OLED output. Second, the above numbers are quoted for virgin devices, but current efficiency decreases and drive voltage typically increases with time of operation, further leading to a reduction in luminous efficiency. Let us assume the OLED is operating at 75% of its virgin luminous efficiency. The combination of these two factors would cause the system luminous efficiency to drop by a factor of 0.3 to 0.9 lm/W, raising the power dissipation to 330 W/m^2.

A considerable further loss in efficiency occurs in passive matrix operation, which is the addressing method used in two system applications to date [9], [10]. In a passive matrix approach, the device is operated in a pulsed mode with low duty cycle and a high peak brightness to give the desired average luminance. For example, in a display such as a monochrome quarter VGA, there are 240 lines, so with a simple architecture the duty cycle for each frame would be about $1/240 = 0.4\%$. Therefore, when on, the device would operate at a current level 240 times higher than a device operated at dc for the same average luminance [9]. Even if this did not degrade the current efficiency, increasing the drive current by a factor of 240 typically will increase the drive voltage by at least a factor of two [5], [6], [9]–[11], reducing the luminous efficiency by an equal amount. In a passive matrix approach for a large-area display, significant power can also be dissipated in the interconnect wires because of the high-current levels which are required due to the low-duty cycles. This power can easily be as large as the power in the OLED's themselves, further dropping the overall system efficiency by a factor of two. Many approaches toward full color, such as white emitters followed by RGB filters or a blue emitter followed by color conversion modules for red and green also inherently imply further energy inefficiencies. Therefore, it is clear that if thermal considerations are not a first order parameter in the system design, the luminous efficiency of the system can drop far below 1 lm/W, and it is easy to design systems on paper with a power density in excess of 1000 W/m^2.
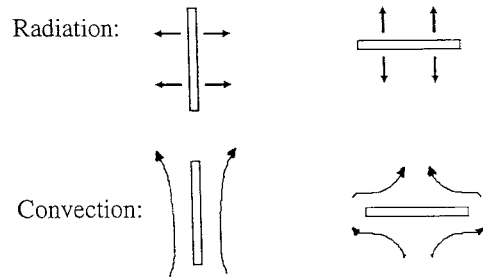

Fig. 1. Schematic diagram indicating thermal dissipation by radiative and convective processes for vertical and horizontal displays.

III. MODELING

An attractive goal is a display with only passive cooling (no fans, thermoelectric coolers, etc.). Such displays may dissipate power though: 1) the emitted light; 2) thermal radiation; 3) or convection; and 4) laterally through the edge of the display (e.g., via the electrical connections on the edge). Because of the low energy efficiencies of organic light emitting devices (OLED's) (<10%), the first mechanism will be ignored in this paper. Furthermore, since in large displays lateral heat conduction will be difficult, the last mechanism will also be ignored in this work, and we will focus on the mechanisms of radiation and convection. We will see that these two mechanisms closely model experimental data for display sizes larger than 1 cm. We will model the display as a thin plate, which may have either a vertical or horizontal orientation (Fig. 1).

The net thermal radiation from a surface does not depend on the orientation of that surface, but it does depend on the temperature and emissivity of the surface. It also depends on the ambient temperature since the surface will absorb some fraction of the radiation from the ambient which is incident upon it. The net power dissipation per unit area (P/A) due to radiation is

$$P/A = \sigma\varepsilon(T_D^4 - T_A^4) = \sigma\varepsilon((T_A + \Delta T_D)^4 - T_A^4)) \quad (2)$$

where T_D is the display temperature, T_A is the ambient temperature, ΔT_D is the rise in the display temperature above that of the ambient, σ is the Stefan–Boltzmann constant, and ε is the emissivity of the display surface. For the relatively small temperature rises in this paper (typically less than 50 K), this may be approximated to be linear with ΔT_D.

$$P/A = 4\sigma\varepsilon T_A^3 \Delta T_D. \quad (3)$$

It is common in heat transfer problems to define a heat transfer coefficient "h" which is the proportionality constant between the power density transferred by a particular mechanism and the temperature rise at a surface.

$$h \equiv (P/A)/\Delta T_D. \quad (4)$$

The heat transfer coefficient for radiation h_r is then

$$h_r = 4\sigma\varepsilon T_A^3. \quad (5)$$

Assuming an emissivity of 0.5 and an ambient temperature of 300 K, h_r is equal to 3.3×10^{-4} W/cm^2·K and is independent of the display size.

The transfer of heat from flat plates by natural convection (i.e., no forced air) has long been studied under the condition that the flat plate is at a uniform temperature. Although that is not exactly true for displays, we will later see data which shows this is a reasonable approximation, and all modeling of convection will be based on such an approximation. In the modeling of convective heat transfer from flat plates [12], [14]–[17], it is conventional to define a dimensionless quantity known as the Rayleigh number (Ra), which itself is the product of two other dimensionless quantities, the Prandtl number and the Grashof number:

$$Ra = GrPr \qquad (6)$$

$$Gr = g\beta\rho^2 L_c^3 \Delta T_D / \mu^2 \qquad (7)$$

$$Pr = \mu c_p / k_a \qquad (8)$$

where β, ρ, μ, c_p, and k_a are the thermal expansion coefficient, density, viscosity, heat capacity, and thermal conductivity of the fluid (e.g., air in our case), respectively, g is the gravitational constant, and L_c is the critical dimension of the plate. For vertical plates, L_c is defined as the height of the plate. For horizontal plates, L_c is defined not simply as the edge but as A/Pe, where A is the plate area and Pe is the plate perimeter [12]. Therefore for a square plate L_c for a horizontal orientation is different from that for a vertical orientation. The difference arises from the actual distance that air must travel across the plate, as can be seen in Fig. 1. The Rayleigh number then depends on the critical size of the display and the temperature rise of the display. In air near room temperature, the Prandtl number $= 0.71$. For this paper, we assumed the following room-temperature (RT) values for the other constants: $\beta = 3.3 \times 10^{-3}$ K^{-1}, $\rho = 1.18 \times 10^{-3}$ g/cm^3, $\mu = 2.16 \times 10^{-4}$ g/cm-s, $c_p = 1.02$ J/g·K and $k_a = 2.6 \times 10^{-4}$ W/cm·K [12], [13].

It is also common to define the dimensionless Nusselt number Nu as

$$Nu = h_c L_c / k_a. \qquad (9)$$

h_c is the convective heat transfer coefficient (analogous to h_r for radiation) which is the proportionality constant between the power density dissipated by convection and the temperature rise of the display. In the heat transfer literature, the Nusselt number is generally given as a function of the Rayleigh number. Thus for a display of a given size and temperature rise one first calculates the Rayleigh number, from which one finds the Nusselt number depending on the geometry in question. From the Nusselt number, one finds the heat transfer coefficient and can thus calculate the power dissipated. Because the power dissipation per unit area will not be exactly uniform over the surface of the display [12], the heat transfer coefficient derived from this method is an average over the entire plate.

Table I shows calculated Rayleigh numbers for vertical plate for sizes from 0.1 to 100 cm and for temperature rises of 1, 10, and 100 K. For Raleigh numbers less than 10^9, the flow of air around the plate is laminar. This encompasses most of the relevant conditions seen in Table I. In this case a boundary layer forms and the diffusion of heat across the boundary layer

TABLE I
CALCULATED RAYLEIGH NUMBER FOR VERTICAL DISPLAYS OF VARIOUS SIZES AND TEMPERATURE RISES ΔT_D ABOVE AMBIENT

Vertical Height (L_c, cm)	Temperature Rise (ΔT_D, K)		
	1	10	100
0.1	0.069	0.69	6.9
0.3	1.9	19	190
1	69	690	6.9×10^3
3	1.9×10^3	1.9×10^4	1.9×10^5
10	6.9×10^4	6.9×10^5	6.9×10^6
30	1.9×10^6	1.9×10^7	1.9×10^8
100	6.9×10^7	6.9×10^8	6.9×10^9

determines the heat transfer. For laminar flow, the Nusselt number generally scales as [12]

$$Nu \alpha Ra^{1/4}. \qquad (10)$$

The heat transfer coefficient then scales as

$$h_c \alpha (\Delta T_D / L_c)^{1/4}. \qquad (11)$$

The heat transfer coefficient increases weakly with the temperature rise of the display and slowly becomes weaker as the display becomes larger. For Raleigh numbers less than about 10^4, although the flow is still laminar, the boundary layer model breaks down, and the Nusselt number has less dependence on the Raleigh number. Thus for small displays with small temperature increases the heat transfer coefficient depends less on temperature but goes down faster as the display size is increased than for moderately larger Rayleigh numbers. For very large Rayleigh numbers (typically above 10^9), the flow become turbulent and the Nusselt number scales as $Ra^{1/3}$, with the result that the heat transfer coefficient becomes independent of size.

For vertical plates of uniform temperature, the Nusselt number has been experimentally fit to the Rayleigh number as [14], [15]

$$Ra < 10^9 : Nu = 0.68 + \frac{0.67Ra^{1/4}}{(1 + (\frac{0.49}{Pr})^{9/16})^{4/9}}$$
$$(12a)$$

$$Ra > 10^9 : Nu = 0.1Ra^{1/3}. \qquad (12b)$$

Note that between the ranges of $10^5 < Ra < 10^9$, this relationship can be modeled more simply by [14]

$$Nu = 0.59Ra^{1/4} \qquad (12c)$$

exhibiting the classical $Ra^{1/4}$ dependence for laminar flow.

For horizontal plates, there is a difference in the heat transfer coefficient from the top and bottom surfaces, with the heat transfer from the top being approximately twice as efficient as that from the bottom. For the top surface [16], [17]

$$Ra < 200 : Nu = 0.96Ra^{1/6} \qquad (13a)$$

$$200 < Ra < 10^7 : Nu = 0.54Ra^{1/4} \qquad (13b)$$

$$10^7 < Ra < 3 \times 10^{10} : Nu = 0.15Ra^{1/3}. \qquad (13c)$$
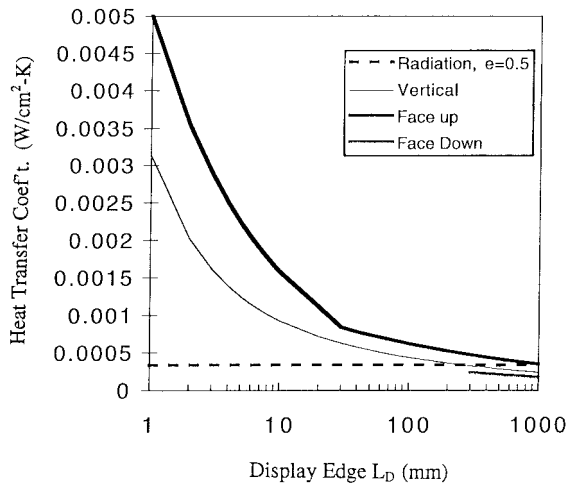
Fig. 2. Modeled average surface heat transfer coefficients as a function of display size L_D for convection for vertical and horizontal (face up and face down) orientations and for radiation (independent of orientation).

For the bottom surface of a horizontal plate [14]

$$3 \times 10^5 < Ra < 3 \times 10^{10}: Nu = 0.27 Ra^{1/4}. \qquad (14)$$

For a comparison of the convective heat transfer coefficients h_c for vertical and horizontal plates and of the radiative heat transfer coefficient (h_r, independent of size), calculated values of these coefficients are plotted versus display size, assuming a temperature rise ΔT_D of 10 K, in Fig. 2. Display size L_D is defined as the vertical edge for a vertical plate (equal to L_c), but equal to four times the ratio of area over perimeter ($4A/Pe$) for a horizontal plate (equal to $4 L_c$). This is done so that a square display has the same x-axis value in the figure for both horizontal and vertical orientations. Note that both radiation and convection are of a similar order of magnitude for large displays. Note also that the heat transfer coefficient falls as the size increases. This occurs especially fast at small dimensions where the Nusselt number has only a weak dependence on the Rayleigh number. Finally, note that the heat transfer coefficients from the surface to the ambient are small, on the order of 10^{-4}–10^{-3} W/cm^2·K.

Because these surface heat transfer coefficients are small, the loss of heat from the display surface is by far the largest thermal resistance in the thermal path from the OLED to the ambient. The largest thermal resistance in the display plate itself will be the resistance of the glass plate. The thermal conductance (inverse of resistance) for heat flow through the glass plate from one side to the other is

$$G_T = k_g/t \qquad (15)$$

where k_g is the thermal conductivity of the glass and t is the glass thickness. k_g is on the order of 0.01 W/cm·K, and assuming a glass thickness of 1 mm, the thermal conductance for heat flow through the glass will be ~0.1 W/cm^2·K. The thermal conductances of any other layers in the OLED structure itself (e.g., the metal and organic layers) will be orders of magnitude higher due the much lower thicknesses of these layers. Because the effective thermal conductance of the interface to the ambient (the surface heat transfer

coefficients) are at least two orders of magnitude lower than the conductance through the glass, the temperature across the glass and OLED device itself will be nearly uniform, with nearly all of the temperature differential to the outside world dropped from the display surface to the ambient. In one case, we developed a numerical model explicitly taking into account all of the thermal resistances in a structure (in a one–dimensional (1-D) approximation). In that example we calculated a temperature differential across the glass of only 0.1 K, even though the temperature rise with respect to the ambient was 23 K. This means that increasing the thermal conductivity of the substrate will have little effect on the display temperature in the case when there is no lateral heat flow, as is expected in large displays.

IV. EXPERIMENTAL RESULTS

In searching the literature, we could find no set of experimental data of the measured temperature rise of flat glass plates as a function of size for different power densities and orientations. Therefore, we conducted a set of experiments using glass plates of 1 mm thickness which were coated on one side with indium tin oxide, which had a sheet resistance of about 15 Ω. The glass was cleaved into different sizes ranging from 3×3 mm^2 to 300×300 mm^2. On two opposite edges of samples, a thin (0.5 mm) strip of solder was placed on top of the indium tin oxide to provide a low-resistance path for sourcing and sinking current, and one thin (<1 mm) wire was connected to each solder strip for an electrical connection. Electrical power was applied to these leads to cause uniform dc power dissipation across the plate. Measurement of the voltage profile across the ITO confirmed the assumption of uniform power dissipation. The plates were then suspended in air in either a horizontal or vertical orientation at a height of about 30 cm above a desk. The plate could thus dissipate heat from both sides. There were no sources of blowing air (vent ducts, fume hoods, cooling fans, etc.) in the room. The temperature in several locations was measured on both sides of the glass plate using a type K thermocouple with 3-mil diameter wires. Several points were also measured using a thermocouple with 10-mil diameter wires. The difference in temperature between the two wire diameters was less than 1 K, so we conclude that there was no significant cooling of the surface caused by heat conduction in the thermocouple itself. The experimental errors in the measured temperature rises above ambient are estimated to about 1 K.

Fig. 3 shows the temperature rise near the center of the back (no ITO) side of two plates in a vertical orientation for a power density of 220 W/m^2 ($\pm 5\%$) as a function of time. To reach steady state a time on the order of 5–10 min is required, with larger displays requiring longer time and reaching a higher final temperature. The steady-state temperature rise was then measured for a power density of 220 W/m^2 at many points on the back surface of plates in both a vertical and horizontal orientation (Fig. 4). There was no significant difference if the horizontal plates had the ITO sides (where the power dissipation is actually occurring) up or down, consistent with the above discussion that the same temperature is expected on
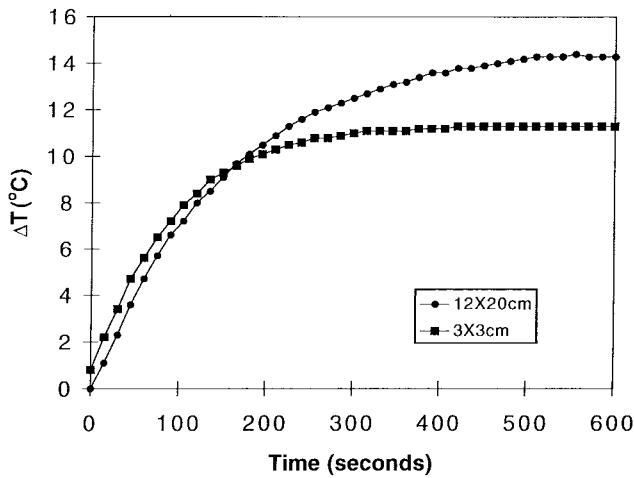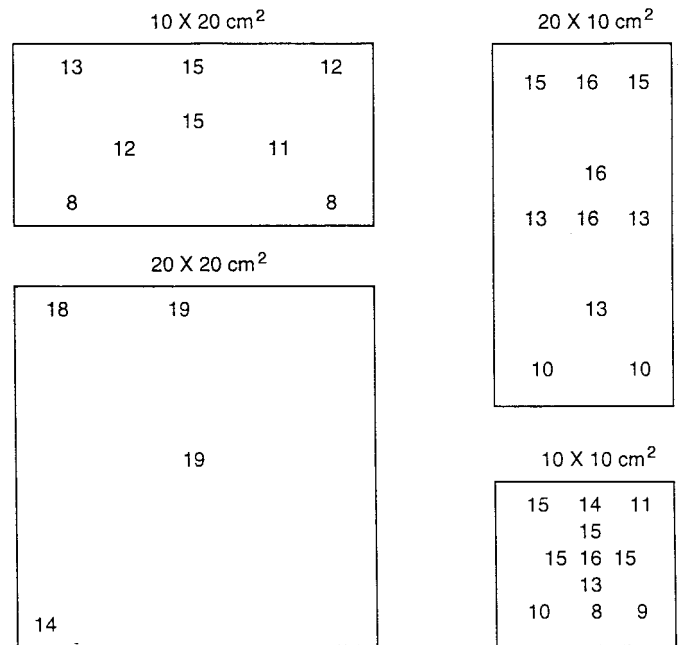
Fig. 3. Temperature rise versus time for a plates near the center of the non-ITO side of plates with vertical orientation of sizes 12 (H) $\times$ 20 (W) cm^2 and 3 $\times$ 3 cm^2 for a power density of 220 W/cm^2.

(a)

(b)

Fig. 4. Map of measured steady-state temperature rises at the center on the non-ITO side of (a) vertical and (b) horizontal (10 $\times$ 10 cm^2) plates of different sizes for a power density of 220 W/cm^2.

either surface. Note that the horizontal plates had the largest temperature rise near the middle. For example, the 10 $\times$ 10 cm plate had a temperature rise of $\sim$18 K near the middle, but only $\sim$14–15 K near the edges. This is expected since most convection loss occurs on the top side [see (13), (14),] and on the top side the air flows from the edge toward the center. The vertical plates were warmest near the top and coolest near the bottom, consistent with the flow of air upwards across the structure. For a 10 cm $\times$ 10 cm plate, the temperature was about 5 K higher near the top than near the bottom, out of a total temperature rise of $\sim$13 K. To first order then we may consider the plate to be at a uniform temperature, which justifies this assumption in the modeling of the previous section.

The dependence of the steady-state temperature rise on power density for two vertical plates is shown in Fig. 5. The rise in temperature is somewhat less than linear. For example, for the 12 cm $\times$ 20 cm plate, the steady-state temperature rise at 220 W/m^2 is 14 K versus 92 K at 2200 W/m^2. This is expected since as noted earlier, convective heat transfer becomes more efficient (a larger h_c) as the temperature rise increases. Near the upper end of the laminar region (Rayleigh numbers $\sim 10^4$–10^9), which includes most of the data in Fig. 5, the heat transfer coefficient is expected to scale as $\Delta T_D^{1/4}$. Radiation also becomes more efficient at larger temperature rises as the linearizing approximation of (3) is no longer valid.

Fig. 6 shows the temperature rise near the middle of the plate at a power of 220 W/m^2 for plates of different sizes and orientations. For vertical plates, this is near the average over the plate surface while for horizontal plates it is near the maximum temperature rise. Points are plotted for both the ITO side of the glass and the bare side (referred to as the "glass" side). First, note that the difference in the two sides is small, as noted earlier. Second, note the horizontal and vertical plates are the same temperature to first order. At first glance this is surprising, since while the Nusselt number (and thus the heat transfer coefficient) of the top side of a horizontal surface is about the same as that from a vertically oriented surface for a given L_C, the bottom face of a horizontally oriented
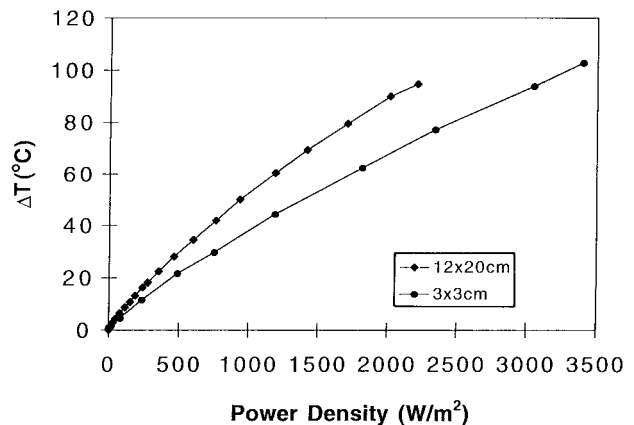

Fig. 5. Steady-state temperature rise in the center of the non-ITO side versus power density for vertical plates of sizes 12 (H) $\times$ 20 (W) cm^2 and 3 $\times$ 3 cm^2.
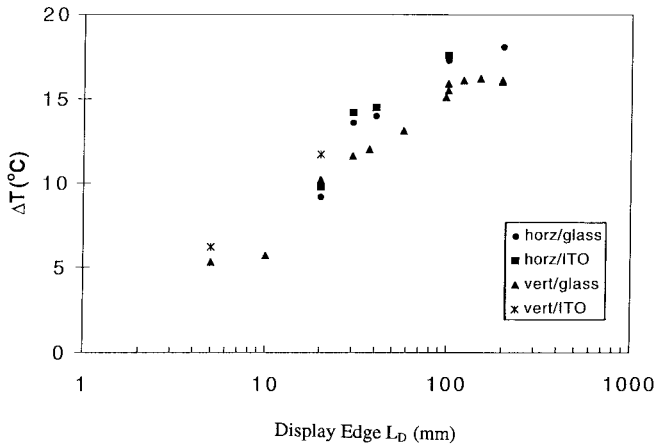
Fig. 6. Steady-state temperature rise in the center of a display as a function of display size L_D for horizontal and vertical orientations.

Fig. 7. Extracted average surface heat transfer coefficients (from the non-ITO side data) as a function of display size L_D for vertical and horizontal orientations.

surface is a factor of two lower [see (12)–(14)]. However, as noted earlier, the critical dimension for convection L_C in the horizontal orientation is less than that of the vertical orientation for a given plate, compensating for the lower average heat transfer coefficient a horizontal surface for the same L_C. Finally, note that the temperature rise has a significant size dependence, increasing from ~5 K for an edge size of 1 cm to ~17 K for an edge size of 30 cm, even though all plates were operated at the same power density. This clearly has implications for the scaling of displays.

V. DISCUSSION AND ANALYSIS

The effective average total surface heat transfer coefficients $h_{\mathrm{avg,tot}}$ were extracted from the data by assuming that the temperature profile across the glass plate is flat, and assuming equal power dissipation from each surface.

$$h_{\mathrm{avg,tot}} \equiv (P/A)/(2\Delta T_D). \tag{16}$$

The factor of two results from the fact that the display plate dissipates power from two surfaces. The points are plotted versus the critical display dimension L_D in Fig. 7. The experimental points surface heat transfer coefficients are on the order of 10^{-3} W/cm²·K, similar to those of the modeling. Fig. 8(a) and (b) compares the predictions of the above modeling to the experimentally measured average surface heat transfer coefficients. A quantitative comparison requires an estimate of the emissivity in the range of 10 um, which is that relevant for the radiation of objects near room temperature. Glass is a good absorber in this range, so for the glass plate we will assume an emissivity of 0.9. Because of a plasma resonance, ITO is typically a good reflector in the infrared [18]. Therefore, for the ITO-coated side of the glass we will assume an emissivity of 0.1. The average emissivity of the two sides is thus 0.5. In calculating the heat transfer coefficient due to convection, one needs to assume a temperature rise (for calculation of the Rayleigh number). Because the experimental data ranged from ~5 to ~18 K, we assumed a temperature rise of 10 K. This is not critical since the heat transfer coefficient is expected to scale at most as $\Delta T_D^{1/4}$ in the laminar range. For vertical displays, the
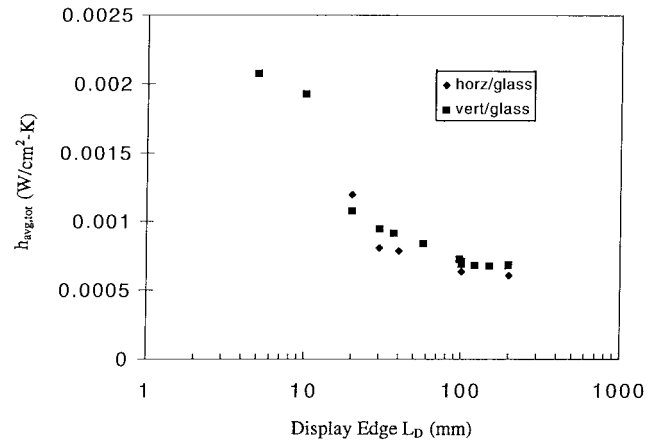
convection on both sides is similar. For horizontal displays, the heat transfer coefficient on the bottom side is half that of the top for the range in which we could find data [see (13), (14)], but this range only applies to plates with edges larger than ~30 cm for a temperature rise of 10 K. Therefore, modeling purposes we assumed that the Nusselt number (and thus the heat transfer coefficient) for the bottom side of a horizontal display was half that of the top side over the entire range relevant to the experimental data. The average convective heat transfer coefficient is then 0.75 of that for the top side. Finally, for both horizontal and vertical plates the total average heat transfer coefficient was defined and plotted as the sum of the average radiation and convective coefficients in Fig. 8(a) and (b).

Fig. 8(a) shows these three modeled lines for the average surface heat transfer coefficients (radiation, convection, and total) along with the experimental points. The data points are in good quantitative agreement with the models for vertical plate edges greater than 1 cm, which are the sizes of technological interest for products. For sizes of 1 cm or less, the models underestimate the heat transfer coefficient and thus overestimate the temperature rise. This may be due to lateral cooling (through the glass plate and then the electrical leads) in the smaller plates. Fig 8(b) shows a similar comparison for the horizontal displays. In this case the models predict about a 20% larger heat transfer coefficient (or 20% smaller temperature increase) than is actually observed for larger sizes. In any case, it is clear that the models presented above reasonably model the steady-state temperature rises of displays under the condition of uniform power dissipation. Given our confidence in the models, one can combine (5)–(9), (12c), and (16) to yield a general equation for the average steady-state temperature rise ΔT_D in a vertically oriented flat-panel display of height L_D with an average surface emissivity ε, both flat sides exposed to ambient air, operating at luminance L:

$$\frac{P}{A} = \frac{\pi L}{\eta_L} = 2.6 \left\{ 4.7\varepsilon + \left(\frac{(\Delta T_D/K)}{(L_D/m)} \right)^{0.25} \right\} \cdot \left(\frac{\Delta T_D}{K} \right) \frac{W}{m^2}. \tag{17}$$
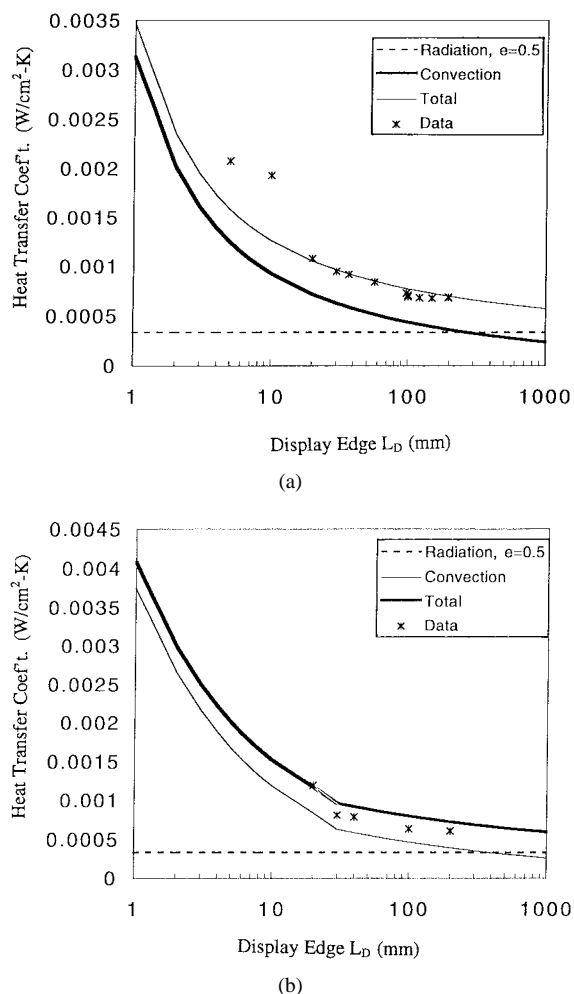
Fig. 8. Comparison of modeled and experimental heat transfer coefficients as a function of display size L_D for (a) vertical and (b) horizontal displays.

In the above equation, L_D is given in meters and ΔT_D is given in degrees kelvin, to yield a result of W/m^2. The factor of π reflects an assumption of Lambertian emission. The above equation is valid for Raleigh numbers between 10^4–10^9, corresponding to $140 < (\Delta T_D/K)\,(L_D/\text{cm})^3 < 1.4 \times 10^7$, which encompasses most conditions of technological interest.

The above data is especially relevant for the scaling of OLED technology in which thermal issues are a primary concern. Many devices fabricated in the lab for reliability testing are on the order of a few mm in size. Extrapolating the data of temperature rise for a power density of 220 W/m^2 in Fig. 6 to 1 mm, one would expect a temperature rise of only $\sim$1 K in such an isolated device. On the other hand, the same device structure at the same power density but of a size of 20 cm would experience a temperature rise nearly 20 times larger. Assuming a similar scaling with power as in Fig. 6, for a power density of 1000 W/m^2 (which is not unrealistic according to the discussion earlier in the paper) the temperature rises for devices of 1-mm and 20-cm size would be about 4 and $\sim$60 K, respectively. The much higher temperature of large devices is an indication that they may have far worse reliability than smaller devices at the same power density.

Our modeling and experiments assumed uniform power dissipation across the plate and that both sides were exposed to the ambient. These are both the most optimistic assumptions one could make. In practice, an OLED display will probably have one surface covered for environmental sealing, and both sides may be further encased in some kind of packaging, contrast enhancing plates, etc. There may be further power dissipation in the package from driver electronics, etc. Further, while a desired luminance such as 100 cd/m^2 is an average over the display surface, the light emitting devices will not cover the entire surface due to space for interconnect wires, isolation between pixels, etc. The actual OLED's will operate at a higher power density and thus a higher temperature than that found in our work for the same average power density (over the entire display surface). On the other hand, cooling fins and high emissivity surfaces (to increase radiation) may lead to temperatures lower than those in our work. Further experiments and two- or three-dimensional (2-D or 3-D) thermal modeling will be required to determine and minimize the display temperature in actual products.

VI. Summary

We have shown that the self-heating of flat-panel displays can be accurately modeled as a combination of radiation and convection. Most significantly, the temperature rise of large displays will be substantially higher than that of small displays, so that that thermal problems become worse as one scales a technology to larger dimensions. This may be especially critical for displays based on OLED's, and thermal issues should be a first-order consideration in display system design. This work also highlights the importance of system luminous efficiency as a primary design criteria for OLED-based products.

References

[1] C. W. Tang and S. A. Van Slyke, "Organic electroluminescent diodes," *Appl. Phys. Lett.,* vol. 51, pp. 913–915, 1987.
[2] J. H. Borroughes, D. D. C. Bradley, A. R. Brown, R. N. Marks, R. H. Friend, P. L. Burn, and A. H. Holmes, "Light-emitting diodes based on conjugated polymers," *Nature,* vol. 347, pp. 539–541, 1990.
[3] D. Braun and A. J. Heeger, "Visible light emission from semiconducting polymer diodes" *Appl. Phys. Lett.,* vol. 58, pp. 1982–1984, 1991.
[4] C. Adachi, S. Tokito, T. Tsutsui, and S. Saito, "Electroluminescence in organic films with three-layer structures," *Jpn. J. Appl. Phys. Lett.,* vol. 27, pt. 2, pp. L269–L271, 1988.
[5] S. A. Van Slyke, C. H. Chen, and C. W. Tang, "Organic electroluminescent devices with improved stability," *Appl. Phys. Lett.,* vol. 69, pp. 2160–2162, 1996.
[6] J. C. Carter, I. Grizzi, S. K. Heeks, D. J. Lacey. S. G. Latham, P. G. May, O. Ruiz de los Paños, K. Pichler, C. R. Towns, H. F. Wittmann, "Operating stability of light-emitting polymer diodes based on poly (p-phenylene vinylene," *Appl. Phys. Lett.,* vol. 71, pp. 34–36, 1997.
[7] P. Burrows, V. Bulovic, S. R. Forrest, L. S. Sapochak, D. M. McCarty, and M. E. Thompson, "Reliability and degradation of organic light emitting devices," *Appl. Phys. Lett.,* vol. 65, pp. 2922–2924, 1994.
[8] C. Adachi, K. Nagai, and N. Tamoto, "Molecular design of hole transport for obtaining high durability in organic electroluminescent diodes," *Appl. Phys. Lett.,* vol. 66, pp. 2679–2681, 1995.

[9] C. Hosokawa, M. Eida, M. Matsuura, K. Fukuoka, H. Nakamura, and T. Kusumoto, "Organic multicolor EL display with fine pixels," in *Dig. Soc. Inform. Display*, May 1997, pp. 1073–1076.

[10] T. Tohma, "Recent progress in development of organic electroluminescent display devices," in *Conf. Rec. Int. Display Research*, Sept. 1997, pp. F-1–F-4.

[11] K. Pichler, S. K. Heeks, C. R. Town, N. T. Harrison, N. Tesler, and R. H. Friend, "Use of sputtered cathodes for polymer light-emitting diodes," *Conf. Rec. Int. Display Research Conf.*, Sept. 1997, pp. F-19–F-22.

[12] B. V. Karlekar and R. M. Desmond, *Heat Transfer.* St. Paul, MN: West, 1977.

[13] R. C. Weast, Ed., *Handbook of Chemistry and Physics,* 54th ed. Cleveland, OH: Chemical Rubber, 1973.

[14] W. H. McAdams, *Heat Transmission*, 3rd ed. New York: McGraw-Hill, 1954.

[15] S. W. Churchill and H. H. S. Chu, *Int. J. Heat & Mass Transfer,* vol. 18, p. 1323, 1975.

[16] R. J. Goldstein, E. M. Sparrow, and D. C. Jones, "Natural convection mass transfer adjacent to horizontal plates," *Int. J. Heat & Mass Transfer,* vol. 16, pp. 1025–1036, 1973.

[17] J. R. Lloyd and W. R. Moran, *ASME*, 1966, Paper 74-WA/HT-66.

[18] K. L. Chopra, S. Major, and D. K Pandya, "Transparent conductors," *Thin Solid Films,* vol. 102, pp. 1–46, 1983.

James C. Sturm (M'80–SM'95) was born in Berkeley Heights, NJ, in 1957. He received the B.S.E. degree in electrical engineering and engineering physics from Princeton University, Princeton, NJ, in 1979, and the M.S.E.E. and Ph.D. degrees in 1981 and 1985, respectively, both from Stanford University, Stanford, CA.

In 1979, he joined Intel Corporation as a Microprocessor Design Engineer. In 1981, he was a Visiting Engineer at Siemens Company, Munich, Germany. In 1986, he joined the faculty of Princeton University in the Department of Electrical Engineering where he is currently a Professor as well as Director of the Center for Photonics and Optoelectronic Materials (POEM). In 1994–1995, he was a von Humboldt Fellow at the Institut für Halbleitertechnik at the University of Stuttgart, Germany. He has worked in the fields of silicon-based heterojunctions, 3-D integration, silicon-on-insulator, optical interconnects, and flat-panel displays. Current research interests include silicon-germanium and related heterojunctions, macroelectronics, flat-panel displays and organic semiconductors.

Dr. Sturm is a member of the IEEE Materials Research Society and the American Physical Society. He was a National Science Foundation Presidential Young Investigator. He has served on the organizing committee of IEDM (1988–1992), as a symposium leader for the Materials Research Society (1987, 1995) and on the SOS/SOI, DRC, and EMC Conference committees. In 1996 and 1997, he has been the technical program chair and general chair of the IEEE Device Research Conference.

Wendy Wilson was born on February 19, 1977. In 1998, she is working towards the B.S. degree in physics and mathematics from the University of Utah, Salt Lake City, where she is presently working on two-particle quantum interactions.

In 1996, she was a member of the Cosmic Ray Group at the University of Utah. In the summer of 1997, she was an intern in the Princeton Summer Institute in the Department of Electrical Engineering at Princeton University, Princeton, NJ, where she worked on experimental studies of heat transfer in flat-panel displays. She will pursue graduate school in theoretical physics after an LDS mission.

Mario Iodice was born in Naples, Italy, in 1965. He receieved the Dr. Eng. degree in electronic engineering in 1991. From 1995 to 1997, he was a Ph.D. student at the Department of Electronic Engineering at the University of Napoli "Federico II," working on modeling and design of silicon electrooptic modulator. During the second half of 1996, he was a visiting Ph.D. student at the Department of Electrical Engineering at Princeton University, where he modeled thermal effects on flat-panel displays.

From 1992 to 1994, he was a scholarship holder at the Research Institute of Electromagnetism and Electronic Components (IRECE-CNR) in Naples, where he was involved on integrated optics and optoelectronics and on laser characterization of electrooptic materials. From August 1993 to September 1994, he was a Visiting Researcher at Delft Institute of Microelectronics and Submicron Technologies, Technical University of Delft, The Netherlands, where he worked on microelectronics technologies and on thermal sensor design. He is now a researcher at IRECE-CNR in Naples, Italy.